



32 The main difference is that in the ocean, background currents are usually not zonal. Moreover, the
33 strongest dynamic processes occur on non-zonal flows or when the initial zonal flow deviates from
34 the zonal direction as observations show (Gnevyshev et al., 2020a, b).

35 One of the central moments in the interaction of Rossby waves and large-scale flows are
36 critical layers. The classical critical layer is not formally attainable for waves. It is the geometric
37 border of the transparency region and the shadow region. The critical layer is defined as $c = U$, i.e.
38 the equality of the longitudinal component of the phase velocity of the wave c and the velocity of
39 the background current U . The critical layers have been studied and are well known for
40 gravitational waves and internal waves (LeBlond, Mysak, 1978). For Rossby waves, the study of
41 the critical layer historically also began with the zonal critical layer.

42 If the background current is strictly zonal, then, as shown in (Gnevyshev et al., 2020a), the
43 determination of the critical layer through the phase velocity is quite correct and can be applied
44 for Rossby waves. However, if the flow is not zonal, such a definition becomes ambiguous and
45 allows Rossby waves to cross the critical layer, with the formation of the so-called overshooting
46 effect. The propagation of Rossby waves on shear flows has its specific feature: the wave track
47 gradually approaches its critical layer, this occurs asymptotically for a long time.

48 One of the features of Rossby waves is the qualitative difference between the problems for
49 the zonal and non-zonal background flow. The first key point that distinguishes the problems of a
50 zonal background flow and a critical layer from a non-zonal one is the number of critical layers.
51 For a strictly zonal flow, there is only one critical layer, while for a non-zonal shear flow, three
52 qualitatively different cases can be distinguished (Gnevyshev et al., 2020a, b) we will consider a
53 bit later. As a consequence, the passage to the limit from a non-zonal flow to a strictly zonal case
54 is nontrivial. In particular, all asymptotic laws under the passage to the limit are of a discontinuous
55 nature (Gnevyshev et al., 2020a, b). In this case, of the three non-zonal critical layers in the passage
56 to the limit, from the non-zonal to the zonal critical layer, only one critical layer remains. And the
57 transition from the zonal to the non-zonal case, in principle, is not possible. As a consequence, a
58 strictly meridional flow acquires the most general character, rather than a purely zonal flow.

59 The second important point for Rossby waves is that the linear operator of Rossby waves
60 ceases to be Hermitian upon passing to the non-zonal case. The adiabatic invariant in the form of
61 the enstrophy conservation law, which exists in the WKB approximation, ceases to hold for non-
62 zonal piecewise linear flow profiles of the "vortex layer" type. A non-zonal strong shear current
63 enters into an active exchange of vorticity with Rossby waves (LeBlond and Mysak, 1978;
64 Fabrikant, 1987; Stepanyants and Fabrikant, 1989; Gnevyshev and Shrira, 1990).



65 The fundamental point in which the analysis of problems for the ocean differs from the
66 atmosphere is the limitedness of ocean currents in space and, as a consequence, in time. Therefore,
67 for the obtained qualitative results of the analysis of the dynamics of Rossby waves to have an
68 applied character, it is important to understand what periods and spatial scales are behind such
69 concepts as "approaching" the critical layer?

70 The classical approach for analyzing the kinematics of waves in dispersive systems is based
71 on the ray equations of Hamilton. However, as is customary even in classical mechanics, no one
72 explicitly solves the differential equations of Hamilton in analytical form. The traditional approach
73 is qualitative and is based on the presence of cyclic variables in the problem. As a rule, these are
74 the longitudinal component of the impulse and the frequency of the wave. If we also use a certain
75 set of symmetries, related to the Hermitian nature of the linear wave operator, then this purely
76 geometric approach suffices to understand qualitatively the evolution of waves on plane-parallel
77 inhomogeneous flows, without solving the ray equations of Hamilton explicitly. Therefore, it is
78 better to use a qualitative method, which is called the isofrequency method. It is based on the
79 geometric construction of isofrequency lines and the concept of the direction of the group velocity.
80 For Rossby waves, a qualitative analysis of the kinematics based on the isofrequency method was
81 performed as early as (Ahmed, Eltaeb, 1980; Duba et al., 2014).

82

83 Based on the fact that asymptotically long adhesion of Rossby waves to the critical layer
84 has already been established, we are trying to understand the specific features of this process. The
85 goal of our work is to determine how real the periods and spatial scales of this process are so that
86 they can be realized for real conditions in the ocean. To answer this question, it is necessary to
87 have explicit analytical solutions for wave tracks as a function of time and initial parameters of the
88 wave disturbance, as well as the magnitude of the shear and the angle of inclination of the flow to
89 the zonal direction. In addition, in this paper, using the example of Rossby waves on a shear flow,
90 we analytically integrate ray equations of Hamilton for the first time. The obtained explicit
91 expressions make it possible to calculate in real-time the Rossby wave tracks for any initial wave
92 direction and any shear current inclination angle. As will be shown below, such tracks for a non-
93 zonal flow are qualitatively highly anisotropic.

94 The generally accepted way to obtain a solution as a function of the initial position of the
95 wave and time is to solve the Cauchy problem. For barotropic Rossby waves, the Cauchy problem
96 was solved in (Yamagata, 1976a, b) for strictly zonal and meridional currents. Continuing this
97 direction, we will show that the integrated ray equations of Hamilton turn out to be equivalent to



98 the asymptotics of the solution of the Cauchy problem. However, in contrast to (Yamagata, 1976a,
99 b), we propose an easier way to obtain explicit analytical expressions for the Rossby wave tracks.
100 To obtain a solution, the introduction of convective coordinates, direct and inverse Fourier
101 transforms, and the stationary phase method for the obtained two-dimensional Fourier integral is
102 not required (Yamagata, 1976a, b). In this work, we will show that ray equations of Hamilton for
103 Rossby waves are integrated with explicit expressions quite simply using the arctangent and
104 logarithm functions, in contrast to the solutions of Yamagata (1976a, b), which use a more specific
105 mathematical apparatus related to the Cauchy problem. The new solutions of the ray equations of
106 Hamilton for Rossby waves are much simpler than the geometric method of isofrequencies and
107 represent explicit analytical expressions for the tracks of Rossby waves in elementary functions.

108

109 2. Results

110 The ray equations of Hamilton are an effective tool for analyzing the kinematic properties
111 of Rossby waves in a plane-parallel shear flow (LeBlond, Mysak, 1978; Salmon, 1998). In
112 practice, this method is often successfully applied in numerical calculations (see, for example,
113 Killworth & Blundell, 2003). We will show that for shear flows there is also an explicit analytical
114 solution of these equations, and these solutions will be found in elementary functions. The so-
115 called equations of geometric optics are as follows:

$$116 \quad k_x = -\frac{\partial \omega}{\partial x}, \quad l_y = -\frac{\partial \omega}{\partial y}, \quad (1)$$

$$117 \quad X_t = \frac{\partial \omega}{\partial k}, \quad Y_t = \frac{\partial \omega}{\partial l} \dots \quad (2)$$

118 Here x and y are the axes of the Cartesian coordinate system directed to the east and north,
119 respectively; t is the time; (k, l) are the components of the wave vector κ , ω is the frequency,
120 $X = X(\omega, k, l)$ and $Y = Y(\omega, k, l)$ are the ray variables in a coordinate system rotated
121 counterclockwise by an angle θ .

122 Let us assume that the background flow is a stationary shear flow directed at a certain angle
123 θ fixed to the parallel. For certainty, we will consider the angle $\theta > 0$ if it is counted
124 counterclockwise. To find a solution, we will proceed as follows. At the first stage, let us go over
125 to the coordinate system associated with the flow. Then in the new coordinate system rotated by
126 the angle θ , the background current velocity field has only one longitudinal velocity component
127 $\vec{U} = (U, 0) = (U(y), 0)$. Further, the coordinate system is chosen so that at its origin the velocity



128 field is zero. Assume that U is approximately linear in y : $U = U_y y$. Having solved the problem in
 129 a new (rotated) coordinate system, we then make a reverse rotation by an angle $(-\theta)$, and thus we
 130 get a solution in the original coordinate system tied to the parallel and the meridian, which is more
 131 convenient for a clear illustration of the result.

132 The dispersion relation in the new coordinate system is (Gnevyshev, 2020a):

$$133 \quad \omega = -\frac{\beta(k \cos \theta - l \sin \theta)}{k^2 + l^2 + F^2} + kU_y y, \quad (3)$$

134 where $\beta = \frac{df}{dy}$, f is the Coriolis parameter, $F^2 = \frac{f^2}{gH}$, g is the acceleration of gravity, H is the
 135 depth of the ocean. In the new coordinate system, there are two cyclic variables; they are the
 136 longitudinal coordinate x and time t . Consequently, the problem has two integrals of motion: the
 137 longitudinal component of the momentum (in the ray approach, this is the x -component of the
 138 wavenumber κ) and the wave frequency ω .

139 The integrated first pair of equations (1) has the form:

$$140 \quad k = k_0 = const, \quad l_c = l_0 - U_y k_0 t, \quad (4)$$

141 where (k_0, l_0) are the initial components of the wavenumber at $t = 0$. Note that the integrated first
 142 pair of the equations of Hamilton gives a result that is identical to the result obtained in the
 143 framework of the Cauchy problem (Gnevyshev et al., 2020a).

144 Integrating Eqs. (2), we find the coordinates of the quasi-monochromatic wave packet, at
 145 the initial moment located at the origin of coordinates:

$$146 \quad Y_\theta = \frac{\beta}{U_y} \left[\frac{\cos \theta - \sin \theta \left(\frac{l_0}{k_0} - U_y t \right)}{k_0^2 + F^2 + (l_0 - k_0 U_y t)^2} - \frac{\cos \theta - \sin \theta \left(\frac{l_0}{k_0} \right)}{k_0^2 + F^2 + l_0^2} \right] \quad (5)$$

$$147 \quad X_\theta = \frac{\beta \cos \theta}{U_y} \left[\frac{k_0}{k_c^3} \left\{ -\arctan \left(\frac{l_c}{k_c} \right) + \arctan \left(\frac{l_0}{k_c} \right) \right\} \right] - \frac{\beta \cos \theta}{U_y k_c^2} \left[\frac{F^2 U_y t + k_0 l_0}{l_c^2 + k_c^2} - \frac{k_0 l_0}{l_0^2 + k_c^2} \right] +$$

$$+ \frac{\beta \sin \theta}{U_y} \left[\frac{1}{2k_0^2} \ln \left(\frac{l_c^2 + k_c^2}{l_0^2 + k_c^2} \right) - \frac{1 - U_y t l_c k_0^{-1}}{l_c^2 + k_c^2} + \frac{1}{l_0^2 + k_c^2} \right] + U_y t Y_c \quad (6)$$



148 The subscript index θ in the solution (X_θ, Y_θ) shows that this solution was found in a coordinate
 149 system rotated counterclockwise by an angle θ . For simplicity, the following notation is
 150 introduced in formula (6):

$$151 \quad l_c = l_0 - U_y k_0 t, \quad k_c = \sqrt{k_0^2 + F^2}. \quad (7)$$

152 Let us turn to dimensionless variables taking into account the Rossby baroclinic radius:

153 $k^* = k_0 / F$, $l^* = l_0 / F$, $k_c^* = k_c / F$, $l_c^* = l_c / F$, $X^* = X_c F$, $Y^* = Y_c F$, and dimensionless
 154 time for the shear of the background flow velocity: $t^* = t |U_y|$. Omitting the asterisks, we get:

$$155 \quad Y_\theta = \frac{\beta}{FU_y} \left[\frac{\cos \theta - l_c k^{-1} \sin \theta}{k_c^2 + l_c^2} - \frac{\cos \theta - l k^{-1} \sin \theta}{k^2 + l^2} \right] \quad (8)$$

$$156 \quad X_\theta = \frac{\beta \cos \theta}{FU_y} \left[\frac{k}{k_c^3} \left\{ -\arctan \left(\frac{l_c}{k_c} \right) + \arctan \left(\frac{l}{k} \right) \right\} - \frac{\beta \cos \theta}{FU_y k_c^2} \left[\frac{k l + t}{l_c^2 + k_c^2} - \frac{k l}{l^2 + k^2} \right] + \right. \\ \left. + \frac{\beta \sin \theta}{FU_y} \left[\frac{1}{2k^2} \ln \left(\frac{l_c^2 + k_c^2}{l^2 + k^2} \right) - \frac{1 - t l_c k^{-1}}{l_c^2 + k_c^2} + \frac{1}{l^2 + k^2} \right] + t Y \right], \quad (9)$$

$$157 \quad \text{where } l_c = l - k t, \quad k_c = \sqrt{k^2 + F^2}, \quad U_y > 0 \quad (10)$$

$$158 \quad \text{and } t \rightarrow -t, \quad U_y < 0. \quad (11)$$

159 This solution can be simply represented as:

$$160 \quad X_\theta = X_1 \cos \theta + X_2 \sin \theta, \quad Y_\theta = Y_1 \cos \theta + Y_2 \sin \theta \quad (12)$$

161 where (X_1, Y_1) is the packet coordinates in the case when the flow is zonal (directed along the
 162 parallel: $\theta = 0$), and (X_2, Y_2) is the packet coordinates in the case when the flow is meridional
 163 (directed along the meridian). It is important to note that $\theta = \frac{\pi}{2}$ for the meridional direction and
 164 the OX_1 axis is directed to the north and the OX_2 is to the west.

$$165 \quad X_1 = \frac{\beta k}{FU_y k_c^3} \left[-\arctan \left(\frac{l_c}{k_c} \right) + \arctan \left(\frac{l}{k} \right) \right] - \frac{\beta}{FU_y k_c^2} \left[\frac{k l + t}{l_c^2 + k_c^2} - \frac{k l}{l^2 + k^2} \right] + t Y_1 \quad (13)$$

$$166 \quad Y_1 = \frac{\beta}{FU_y} \left[\frac{1}{k_c^2 + l_c^2} - \frac{1}{k^2 + l^2} \right], \quad (14)$$



$$167 \quad X_2 = \frac{\beta}{FU_y} \left[\frac{1}{2k^2} \ln \left(\frac{l_c^2 + k_c^2}{l^2 + k_c^2} \right) - \frac{1 - tl_c k^{-1}}{l_c^2 + k_c^2} + \frac{1}{l^2 + k_c^2} \right] + tY_2, \quad (15)$$

$$168 \quad Y_2 = \frac{\beta}{FU_y} \left[\frac{lk^{-1}}{l^2 + k_c^2} - \frac{l_c k^{-1}}{l_c^2 + k_c^2} \right] \dots \quad (16)$$

169 Then, designating the coordinates of the package in the coordinate system tied to the east and north
170 directions (X , Y), you need to reverse the rotation of the coordinate system (counterclockwise).
171 Finally, we get the following expressions in a matrix form:

$$172 \quad \begin{pmatrix} X \\ Y \end{pmatrix} = \begin{pmatrix} \cos \theta & -\sin \theta \\ \sin \theta & \cos \theta \end{pmatrix} \begin{pmatrix} X_\theta \\ Y_\theta \end{pmatrix} \quad (17)$$

173 or

$$174 \quad X = X_1 \cos^2 \theta + (X_2 - Y_1) \cos \theta \sin \theta - Y_2 \sin^2 \theta \quad (18)$$

$$175 \quad Y = Y_1 \cos^2 \theta + (X_1 + Y_2) \cos \theta \sin \theta + X_2 \sin^2 \theta \quad (19)$$

176 3. Numerical estimation of dimensionless parameters

177 We will take as the initial the following characteristic physical scales for the ocean:

178 $f = 10^{-4} \text{ s}^{-1}$, $\beta = 10^{-11} \text{ m}^{-1} \text{ s}^{-1}$, $F = 0.5 \times 10^{-5} \text{ m}^{-1}$. Some numerical estimates give something like this:
179 whereas we take for the scale of the background flow velocity $U = 5 \text{ cm / s}$, and the scale of the
180 background flow variability 50 km, then the unit of the dimensionless time scale U_y^{-1} is about 11
181 days. Therefore, the dimensionless time $t = 2.86 \times \pi$ is about 3 months. In this case, the
182 dimensionless parameter $\frac{\beta}{U_y F}$ is equal to 0.5. Whereas we take 100 km as the scale of the
183 background flow variability, then the unit of the dimensionless time scale U_y^{-1} is approximately 22
184 days. Then the dimensionless time $t = 2.86 \times \pi$ is about 6 months, and the dimensionless parameter
185 $\frac{\beta}{U_y F}$ is equal to 1.0. These estimates make the results obtained physically justified and correct
186 for practical use.

187 4. Graph analysis

188 Qualitatively, all plots can be divided into two cases: for zonal flow (Fig. 1) and non-zonal
189 (Fig. 2). A common property of all graphs is that with increasing time, all rays adhere to the critical
190 layer. However, the number of critical layers, as well as their location, is a nontrivial function of



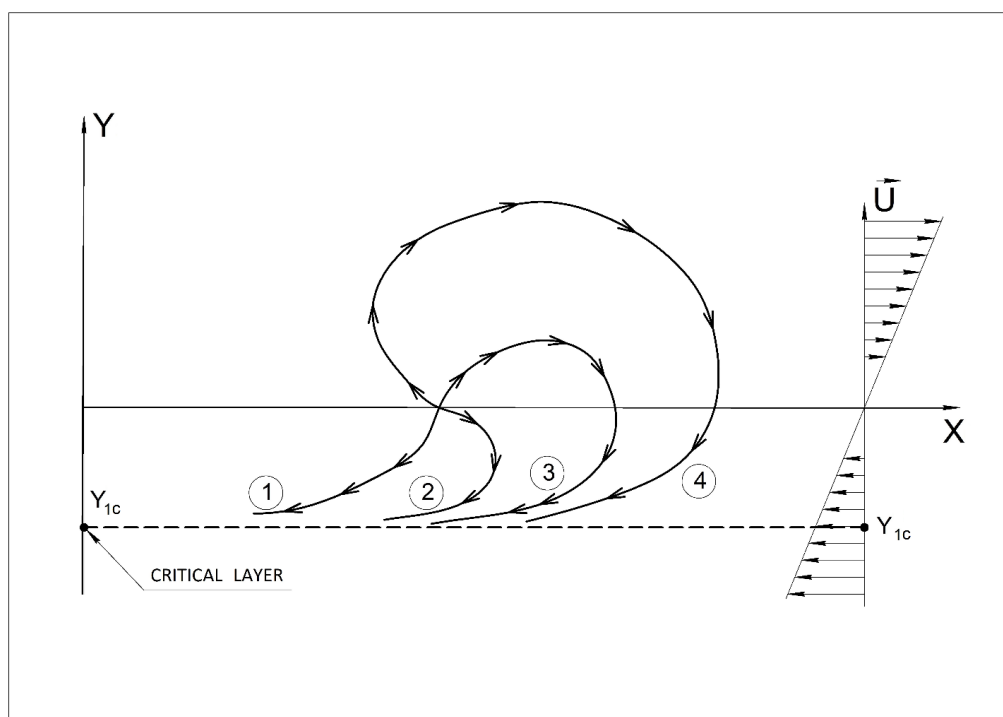
191 the angle of inclination of the background flow. Qualitatively, several main scenarios can be
192 distinguished.

193 *Zonal flow scenario.* If the flow is strictly zonal, $\theta = 0$ (Fig. 1), then one critical layer is
194 formed, which does not depend on the initial direction of the group velocity and is determined only
195 by the magnitude of the modulus of the initial wavenumber. The expression for the ordinate of the
196 critical layer is determined by the following (nonzero) value:

$$197 \quad Y_{1c} \Big|_{t \rightarrow \infty} \rightarrow -\beta \left(F U_y \left[k_c^2 + l_0^2 \right] \right)^{-1} \quad (20)$$

198 In the case of a strictly zonal flow, all waves adhering to the critical layer move strictly to
199 the west: $X_{1c} \Big|_{t \rightarrow \infty} \rightarrow -\infty$. It is also important to note that the movement of Rossby waves at certain
200 points in time is possible both to the east and in other directions. However, with increasing t , all
201 rays adhere to the critical layer, moving strictly to the west. An analysis of the tracks shows that
202 the dimensionless time values at which the movement begins to follow a strictly westerly direction
203 is approximately $t = 8$, and it gives a period of about three months for the open ocean.

204 In the case of a zonal flow, the initial component of the group velocity in the meridional
205 direction is proportional to $k_0 \times l_0$. For the zonal component of the group velocity, the sign is
206 determined by the following expression: $(k_0^2 - l_0^2 - 1)$. To have an idea of all possible cases, it
207 suffices to take the following set of four initial wavenumbers (k_0, l_0) . Figure 1 shows four options
208 for the initial direction of the group velocity; the tracks are drawn for the case $U_y > 0$. The abscissa
209 axis is directed to the east, the ordinate is to the north. Track 1 – the initial group velocity is directed
210 to the southwest. The initial components of the wavenumber are $k_0 = -1, l_0 = 1$. Track 2 – the initial
211 group velocity is directed to the southeast: $k_0 = -4\sqrt{2} / \sqrt{17}, l_0 = \sqrt{2} / \sqrt{17}$ or $k_0 = -1.372, l_0 =$
212 0.343 . Track 3 – the initial group velocity is directed to the north-east:
213 $k_0 = -4\sqrt{2} / \sqrt{17}, l_0 = -\sqrt{2} / \sqrt{17}$ or $k_0 = -1.372, l_0 = -0.343$. Track 4 – the initial group velocity
214 is directed to the northwest: $k_0 = -1, l_0 = -1$. The wavenumbers are specially selected so that the
215 tracks adhere to one critical layer. For all four combinations, the relation $k_0^2 + l_0^2 + 1 = 3$.



216

217 Fig. 1. The variety of tracks of Rossby waves in their interaction with the zonal flow.

218 Descriptions of tracks 1 - 4 are given in the text.

219 *Non-zonal flow scenario.* For a strictly meridional flow $\theta = \frac{\pi}{2}$, there are three qualitatively
 220 different cases for the implementation of the critical layer, which can be conventionally called
 221 "positive", "negative" and "zero". For the case of a strictly zonal flow, the critical layer is the
 222 boundary of the transparency region. For any non-zonal flow, additional critical layers appear that
 223 are inside the transparency region. The critical layer is "negative", for which the sign of the
 224 intrinsic frequency adhering to the critical layer is negative. Such waves with a negative intrinsic
 225 frequency are commonly called "waves of negative energy" (Fabrikant, Stepanyants, 1998). The
 226 peculiarity of the non-zonal case is that Rossby waves, starting from zero value, can change the
 227 sign of their intrinsic frequency at a certain moment in time.

228 The expression for the ordinate of the critical layer is determined by the following value.

229
$$Y_{2c} \Big|_{l_0 \rightarrow \infty} \rightarrow \frac{l_0}{k_0 U_y} \left[\frac{\beta}{F [k_c^2 + l_0^2]} \right] \quad (21)$$



230 Recall that the coordinate system is tied to the direction of the flow velocity, so in this case,

231 when $\theta = \frac{\pi}{2}$, the x -axis is directed to the north and the y -axis to the west.

232 Group speed signs are defined as follows:

$$233 \quad C_{grx} \approx (-kl), \quad C_{gry} \approx (k^2 + 1 - l^2).$$

234 Consider the case $U_y > 0$. Provided $lk^{-1} > 0$, waves adhere to the negative critical layer:

235 ($Y_{2c} > 0$). Wherein $X_{2c}|_{l \rightarrow \infty} \rightarrow -\infty$, and the value of the group velocity along the x -coordinate
236 turns out to be negative. That is, it turns out that for adhesion to the negative critical layer, the
237 wave must start against the direction of the flow, but the flow will certainly turn the wave in the
238 direction of the flow. The wave will cross the critical layer, change the sign of its intrinsic
239 frequency, reflect from the higher value of the background flow velocity, and start again
240 approaching the critical layer, but from the opposite side. This wave behavior is called
241 overshooting (see Gnevyshev et al., 2020a); it also occurs in quantum mechanics.

242 For the initial values ($k_0 = 1, l_0 = 1$), the direction of the group velocity has the opposite
243 direction with respect to the flow, and a negative critical layer is realized. Whereas for the initial
244 values ($k_0 = -1, l_0 = 1$), the direction of the group velocity coincides with the direction of the flow,
245 and the negative critical layer is not realized. Reflection occurs, and the wave goes to the positive
246 critical layer.

247 Provided $l_0 k_0^{-1} < 0$, waves adhere to the positive critical layer, ($Y_{2c} < 0$). The situation is
248 qualitatively similar to the purely zonal case. In this case, the critical layers have not only
249 components of different signs and magnitude, but also tend to $\pm\infty$ by the x -coordinate,
250 ($X_{2c} \rightarrow -\infty$).

251 From the analysis of these ratios, it can be seen that an additional second critical layer,
252 which appears due to the non-zoning of the flow, is realized only for waves that initially fall strictly
253 against the current. Whereas waves that fall in the direction of the flow have a trivial reflection
254 from the negative critical layer. Let us also note the existence of a third scenario. At $l_0 = 0$, the
255 wave starts strictly perpendicular to the background current, while the critical layer ($Y_{2c} = 0$) is
256 zero.

257 Let us analyze the intermediate flow direction. The asymptotics for the ordinate of the
258 critical layer in the general case has the form:



$$259 \quad Y_{\theta}|_{l \rightarrow \infty} \rightarrow \frac{l_0 \sin \theta - k_0 \cos \theta}{k_0 U_y} \left[\frac{\beta}{F(k_0^2 + l_0^2)} \right] \dots \quad (22)$$

260 The longitudinal component of the group velocity is proportional to

$$261 \quad (k_0^2 - l_0^2 - 1) \cos \theta - 2k_0 l_0 \sin \theta .$$

262 The transverse component of the group velocity is proportional to

$$263 \quad 2k_0 l_0 \cos \theta - (l_0^2 - k_0^2 - 1) \sin \theta .$$

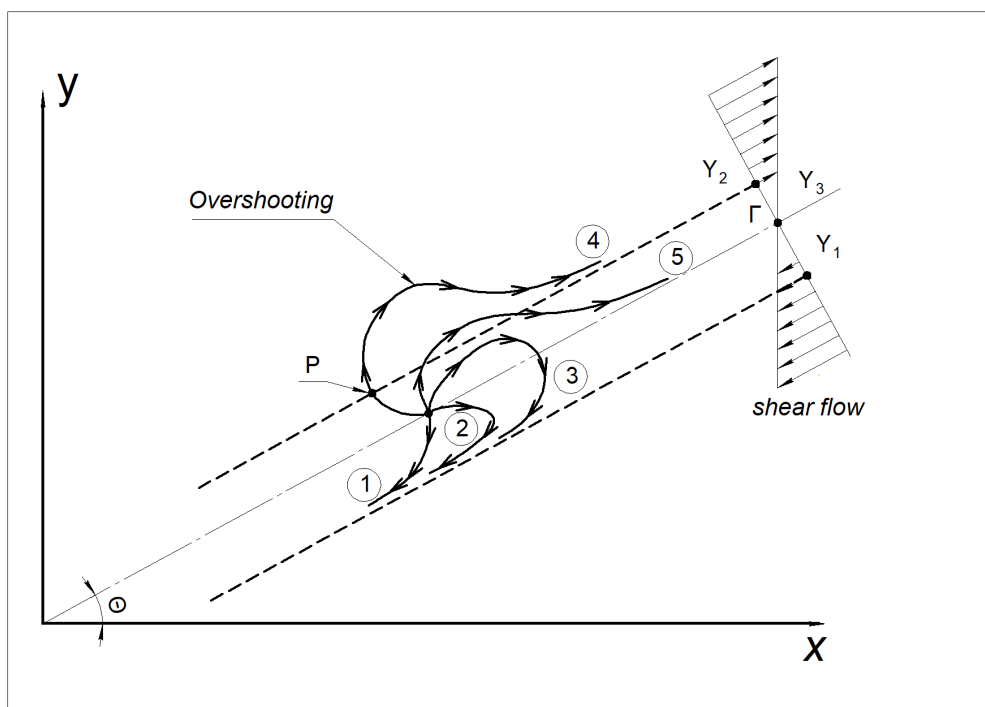
264 It follows from expression (22) that when even weak non-zonality appears, there is not one,
265 as in the case of a purely zonal flow, but three critical layers since the value $(l_0 \sin \theta - k_0 \cos \theta)$
266 can be positive or negative values or zero. For zonal flow, regardless of the parameters of the
267 wavenumber of the incident wave, any wavenumbers can be considered, however, the critical layer
268 is always at negative velocities. For a non-zonal flow at different wavenumbers, that is, at different
269 angles of incidence on the flow, there will be three such critical layers: one at a negative velocity
270 value, one at a positive velocity value, and one with zero velocity. If we fix the wavenumber, then
271 there is always one critical layer. For a zonal flow, this layer will correspond to a negative velocity
272 value. For non-zonal flow, there are possible options: the critical layer will be located either at a
273 positive velocity value or at a negative one or with zero velocity. In other words, some
274 wavenumbers will stick to the positive, and others to the negative values of the background
275 velocity. When we say "one critical layer", we do not mean a fixed value of the velocity, but only
276 its sign.

277 The first critical layer that is implemented for western propagation is the classic well-
278 known and well-studied critical layer for Hermitian operators. The second critical layer is realized
279 for waves moving eastward. This critical layer does not have symmetries due to the non-Hermitian
280 nature of the non-zonal linear operator of Rossby waves and introduces such a phenomenon as
281 overshooting into the kinematics of Rossby waves. The third critical is zero and is inherent only
282 in strictly non-zonal flows. In this scenario, the waves return to the initial level from which they
283 started.

284 For simplicity of numerical values, we take the angle $\theta = \frac{\pi}{4}$. Then we have the following
285 typical sets of wave tracks: track 1 – $(k_0 = -0.5, l_0 = 1)$; track 2 – $(k_0 = -1, l_0 = 1)$; track 3 – $(k_0 = -$
286 $2, l_0 = -0.5)$; track 4 – $(k_0 = -1, l_0 = -2)$; track 5 – $(k_0 = -1, l_0 = -1)$. Such a variety of possible
287 scenarios is inherent precisely in Rossby waves and is associated with the absence of symmetries



288 in the problem, which are a consequence of the non-Hermitian nature of the linear operator of
289 Rossby waves for arbitrary shear flows.



290

291 **Fig. 2.** The variety of Rossby wave tracks in their interaction with the non-zonal current. The
292 description of tracks 1 - 4 is given in the text.

293

294 Discussion and Conclusions

295 The ray equations of Hamilton are a kind of approximate method for analyzing the
296 kinematics of waves. Therefore, a question arises: what are the limits of applicability of these
297 equations?

298 To answer this question, we will proceed from the statement that, from a mathematical
299 point of view, the solution of the Cauchy problem is more correct than the ray equations of
300 Hamilton. The solution of the Cauchy Problem for Rossby waves on a shear plane-parallel flow,
301 in a coordinate system associated with the flow and directed at a certain angle θ to parallel, has
302 the form (Gnevyshev et al., 2020a, b):



$$\begin{aligned}
 303 \quad \Psi(x, y, t) &= \int_{-\infty}^{+\infty} \int_{-\infty}^{+\infty} G(k, l) \frac{(k_z^2 + l^2)}{(k_z^2 + l_t^2)} \times \exp(iY(x, y, k, t)) dk dl, \\
 304 \quad Y(x, y, k, l, t) &\equiv \frac{\beta \cos \theta}{U_y k_z} \left\{ -\arctan\left(\frac{l_t}{k_z}\right) + \arctan\left(\frac{l}{k_z}\right) \right\} + \frac{\beta \sin \theta}{2U_y k} \ln\left(\frac{k_z^2 + l_t^2}{k_z^2 + l^2}\right) + \\
 &+ \left[k(x - U_y t) + ly \right] \quad (23)
 \end{aligned}$$

305 where the following designations are introduced: $l_t = l - U_y kt$, $k_z = \sqrt{k^2 + F^2}$. We construct the
 306 phase for the solution in the form of the ray equations as follows:

$$307 \quad \Theta(x, y, k, l, t) = -\int \omega dt \quad (24)$$

308 Let us substitute in (24) the expression for the frequency (3) and the first pair of integrated
 309 equations (4). In this case, using the free term in the form of an arbitrary function of the
 310 wavenumbers, we normalize the phase as follows: $\Theta(y, k, l, t)|_{t=0} = 0$. Integrating (24) with the
 311 chosen normalization conditions, we obtain:

$$\begin{aligned}
 312 \quad \Theta(y, k, l, t) &= -\int \left\{ \frac{-\beta(\kappa_0 \cos \theta - l_c \sin \theta)}{\kappa_0^2 + l_c^2 + F^2} + \kappa_0 U_y y \right\} dt = \\
 &= \frac{\beta \cos \theta}{U_y \kappa_z} \left\{ -\arctan\left(\frac{l_c}{\kappa_z}\right) + \arctan\left(\frac{l_0}{\kappa_z}\right) \right\} + \frac{\beta \sin \theta}{2U_y \kappa_0} \ln\left(\frac{\kappa_c^2 + l_c^2}{\kappa_c^2 + l^2}\right) - \kappa_0 U_y y t \quad (25)
 \end{aligned}$$

313 Comparing the obtained expression (25) for the normalized phase of the WKB-solution with the
 314 expression for the phase of solution (23) of the Cauchy problem, we find the following relation:

$$315 \quad \Theta(y, k, l, t) + kx + ly = Y(x, y, k, l, t).$$

316 Thus, the phases of the solutions coincide. On the other hand, if we assume that the scale of
 317 changes in the main flow is much larger than the characteristic scale of the solution for
 318 perturbations, then a small parameter ε will appear in the problem (Gnevyshev et al., 2019, 2021),
 319 which formally, after reduction to dimensionless form, is expressed by replacing the derivative the
 320 main flow velocity U_y by $\varepsilon \times U_y$. Passing in the expression for the phase of solution (23) to the limit
 321 in U_y , as in a small parameter, and keeping the zero and first terms of the expansion, we obtain the
 322 following relation:

$$323 \quad Y(x, y, k, l, t)_{(U_y \rightarrow 0)} \rightarrow \left(\frac{-\beta(\kappa \cos \theta - l \sin \theta)}{\kappa^2 + l^2 + F^2} + \kappa U \right) t + \kappa x + ly = \omega t + \kappa x + ly,$$



324 where $\omega = \frac{-\beta(\kappa \cos \theta - l \sin \theta)}{\kappa^2 + l^2 + F^2} + \kappa U$.

325 On the other hand, from (23) it is easy to obtain the following relation:

326 $\lim_{(U, t \rightarrow \infty)} Y(x, y, k, l, t) \neq \omega t + \kappa x + l y$

327 Summing up, let us emphasize the first original result obtained in this work. Solutions (5)
328 and (6) obtained in the framework of the Cauchy problem are exact solutions of ray equations (1)
329 and (2). Consequently, not only do the limiting values obtained within the framework of the WKB-
330 solution and the Cauchy problem in the first approximation coincide, but also the solutions
331 themselves. In other words, the integral of the solution phase, obtained in the first order of the
332 WKB approximation and normalized to zero at the initial moment of time, coincides with the phase
333 of the basic solution of the Cauchy problem. In this case, the expansion of the phase of the solution
334 of the Cauchy problem in terms of the small WKB-parameter in the first approximation gives the
335 dispersion relation obtained in the first order of the WKB-solution. For large time intervals, the
336 phase of the solution to the Cauchy problem does not reach the WKB-solution mode. Hence, from
337 the point of view of the Cauchy problem, the WKB-solution cannot work up to any infinitely large
338 times with a finite shear of the background flow velocity profile.

339 Otherwise, it can be explained as follows. The time t and the shear of the background
340 current velocity U_y are included in the solution in the form of the product $t \times U_y$. Consequently,
341 whatever the small parameter U_y , there will come a time t such that the product $t \times U_y$ will be
342 greater than one, and the series expansion of the solution phase will no longer be justified.

343 Thus, the application of the Hamiltonian formalism in a linear problem helps to build a
344 bridge between seemingly different solutions obtained in the WKB-approximation and the
345 framework of the Cauchy problem. In this case, the first pair of ray equations (1) is nothing but
346 the condition of equality of the cross derivatives of the solution phase. The second pair of ray
347 equations (2) is the equation for a stationary point. The mathematical reason for this behavior is
348 that in the presence of non-zoning in the solution phase, a logarithm of the form appears
349 $\ln(1 + U_y^2 t^2)$. The Taylor series of the logarithm at zero has a radius of convergence equal to one.
350 Consequently, no matter how small the value of the shear in the profile of the background flux U_y
351 is, there will come a time at which the argument of the logarithm will exceed one and the
352 asymptotic expansion will stop working.

353 In this paper, using the example of Rossby waves on non-zonal shear flows, explicit
354 analytical integration of the ray equations of Hamilton is performed for the first time. Previously,



355 no one paid attention to this possibility. It turned out that the obtained explicit analytical solution
356 of ray equations of Hamilton is expressed in simple elementary functions, which turned out to be
357 quite unexpected. The constructed typical kinematic tracks of Rossby waves on non-zonal shear
358 currents show the relevance of such a phenomenon as the critical layers of Rossby waves.

359 In its simplicity and ease, this method surpasses the solution in terms of the Cauchy
360 problem using convective coordinates, and from an analytical point of view, it is identical to the
361 asymptotics of the two-dimensional integral of the Cauchy problem that we obtained earlier
362 (Gnevyshev et al., 2020a).

363 An analytical comparison of the obtained solution with the solution of the Cauchy problem
364 for Rossby waves is made. For small time intervals, the solutions of the ray equations strictly
365 coincide with the asymptotics of the integral obtained in the framework of the Cauchy problem.
366 The non-zonality of the flow leads to the appearance of a logarithm in the solution phase, which
367 greatly complicates the convergence of the results obtained. At large time intervals, the non-
368 zonality of the flow leads to a logarithmic spreading of the solution, which requires additional
369 analysis within the framework of the convolution of the obtained solutions over the spectrum of
370 wavenumbers.

371 The obtained analytical expressions were used to construct the kinematic tracks of Rossby
372 waves on shear flows. The solutions are anisotropic and, in the general case, do not have classical
373 north-south symmetries.

374 It is shown that in the non-zonal case, a second critical layer is added to the classical critical
375 layer of Rossby waves for the strictly zonal case, which is directly related to such concepts as
376 negative energy waves and overshooting.

377 **Acknowledgements**

378 The publication was funded by the Russian Science Foundation, project No 22-27-00004.

379 **Author Contributions**

380 VG presented the idea, made theoretical analysis, wrote the paper draft. TB plotted figures,
381 wrote and edited the manuscript. All authors have read and agreed to the published version of the
382 manuscript.

383 **Funding**

384 The publication was funded by the Russian Science Foundation, project No 22-27-00004.



385 **Compliance with Ethical Standards**

386 **Conflict of interest**

387 The authors declare that they have no conflicts of interest.

388 **References**

- 389 1) Ahmed, B. M., & Eltaeb, I. A. 1980. On the propagation, reflexion, transmission and
390 stability of atmospheric Rossby-gravity waves on a beta-plane in the presence of
391 latitudinally sheared zonal flows. *Philosophical Transactions of the Royal Society of*
392 *London. Series A, Mathematical and Physical Sciences*, 298 (1435), 45–85. doi: 10.1098 /
393 rsta.1980.0240.
- 394 2) Duba, C. T., Doyle, T. B., & McKenzie, J. F. 2014. Rossby wave patterns in zonal and
395 meridional winds. *Geophysical & Astrophysical Fluid Dynamics*, 108 (3), 237–257.
396 <http://dx.doi.org/10.1080/03091929.2013.867604>.
- 397 3) Fabrikant, A. L., & Stepanyants, Yu. A. 1998. Propagation of waves in shear flows. *World*
398 *Scientific*, Singapore, 287 p.
- 399 4) Fabrikant, A. L. 1987. Reflection of Rossby waves from the surface of the tangential
400 velocity discontinuity. *Izvestiya Akademii Nauk SSSR, Fizika Atmosfery i Okeana*, 23,
401 106-109 (In Russian).
- 402 5) Fu, L.-L., & A. Cazenave. 2000. *Satellite Altimetry and Earth Sciences: A Handbook of*
403 *Techniques and Applications*. San Diego, CA: Academic Press.
- 404 6) Gnevyshev, V. G., Badulin, S. I., & Belonenko, T. V. 2020a. Rossby waves on non-zonal
405 currents: structural stability of critical layer effects. *Pure Appl. Geophys.* 177(11), 5585-
406 5598. doi: 10.1007/s00024-020-02567-0.
- 407 7) Gnevyshev, V. G., Badulin, S. I., Koldunov, A. V., & Belonenko, T. V. 2020b. Rossby
408 Waves on Non-zonal Flows: Vertical Focusing and Effect of the Current Stratification.
409 *Pure Appl. Geophys.* 178(8), 3247-3261. <https://doi.org/10.1007/s00024-021-02799-8>.
- 410 8) Gnevyshev, V. G., Frolova, A. V., Koldunov, A. V., & Belonenko, T. V. 2021.
411 Topographic Effect for Rossby Waves on a Zonal Shear Flow. *Fundamentalnaya i*
412 *Prikladnaya Gidrofizika.*, 14, 1, 4-14. doi: 10.7868/S207366732101001.
- 413 9) Gnevyshev, V. G., & Shrira, V. I. 1990. On the evaluation of barotropic-baroclinic
414 instability parameters of zonal flows on a beta-plane. *Journal of Fluid Mechanics*, 221,
415 161-181. <https://doi.org/10.1017/S0022112090003524>
- 416 10) Gnevyshev, V. G., Frolova, A. V., Kubryakov, A. A., Sobko, Yu. V., & Belonenko, T. V.,
417 2019. Interaction between Rossby Waves and a Jet Flow: Basic Equations and Verification



- 418 for the Antarctic Circumpolar Current. *Izvestiya, Atmospheric and Oceanic Physics*, 55
419 (5), 412-422. DOI 10.1134 / S0001433819050074
- 420 11) Killworth, P. D., & Blundell, J. R. 2003. Long extratropical planetary wave propagation in
421 the presence of slowly varying mean flow and bottom topography. Part I. The local
422 problem. *Journal of Physical Oceanography*, 33 (4), 784-801. doi:10.1175/1520-
423 0485(2003)33<.
- 424 12) LeBlond, P. H., & Mysak, L. A. 1978. *Waves in the Ocean*. Elsevier Scientific Publishing
425 Company. 602.
- 426 13) Pedlosky, J. 1979. *Geophysical Fluid Dynamics*. NY: Springer-Verlag. 624 p.
- 427 14) Rossby, C. G., et al. 1939. Relation between variations in the zonal circulation of the
428 atmosphere and the displacements of the semi-permanent centers of action. *J. Mar. Res.* 2:
429 38-55.
- 430 15) Salmon, R. 1998. *Lectures on Geophysical Fluid Dynamics*. Oxford University Press; 1st
431 ed. 392 p.
- 432 16) Stepanyants, Y. A., & Fabrikant, A. L. 1989. Propagation of waves in hydrodynamic shear
433 flows. *Uspekhi Fizicheskikh Nauk*, 32, 783–805,
434 <https://doi.org/10.1070/PU1989v032n09ABEH002757>. (in Russian).
- 435 17) Yamagata, T. 1976a. On the propagation of Rossby waves in a weak shear flow. *Journal*
436 *of the Meteorological Society of Japan*, 54 (2), 126-127.
- 437 18) Yamagata, T. 1976b. On trajectories of Rossby wave-packets released in a lateral shear
438 flow. *Journal of the Oceanographic Society of Japan*, 32, 162-168.